SINGLE BASIN DOUBLE SLOPE SOLAR STILL – YEAR ROUND PERFORMANCE PREDICTION FOR LOCAL CLIMATIC CONDITIONS AT SOUTHERN INDIA

by

Kalidasa Murugavel KULANDAIVEL*[a] *and Srithar KARUPPIAH*[b]

[a] Centre for Energy Studies, National Engineering College, K. R. Nagar, Kovilpatti, Tamil Nadu, India
[b] Department of Mechanical Engineering, Thiagarajar College of Engineering, Madurai, Tamil Nadu, India

Original scientific paper
DOI: 10.2298/TSCI120517109K

In this work, performance of a single basin double slope solar still has been studied theoretically and experimentally. The theoretical model is used to predict the year round performance of the still at the local climatic conditions for the year 2008. Average values of maximum and minimum atmospheric temperatures, wind velocities were taken from meteorological data for last five years. Radiation models were used to predict the global and diffused irradiances on the inclined covers. The time to time variations in transmittance of the cover were considered. The rate of production variation and the total production for first day of the every month had been calculated. The overall production of the still was higher during March, April, August, November, and December and it is around 4 L/day. The average production of the still was 2.1 L/day/m^2*. The economy of the still was also studied and the payback period of the still was three years.*

Key words: *solar still, theoretical analysis, experimental analysis, transmittance variations, performance prediction, year round performance*

Introduction

Drinking water is still a big problem in most arid and remote areas. Single basin solar still is a valuable solution for this problem. This type of still is capable of producing clean potable water from available brackish or wastewater throughout the year. Single slope still is suitable at higher latitude place, while at lower places double slope still is preferred [1]. For theoretical analysis, the transmittance of the cover plate is assumed as constant [2-7] and the irradiance on the horizontal basin area is taken as energy input [2, 3, 5-7]. However, the transmittance of the cover depends on many parameters like incidence angle, cover plate material and its thickness [8]. Only few authors have considered this effect during the analysis [9-11]. Experiments have been conducted by Kalidasa Murugavel *et al*. [12] with different thicknesses of commercially available window glasses at different inclination, orientation and radiation conditions. Correlation has been obtained to estimate the transmittance of the given glass at any place, time, inclination, and orientation. From the above experimental results, it is learnt that, for given glass cover, the transmittance is a strong function of solar angle of incidence (AOI) for most of the daytime. However, during morning and evening, the transmittance of the cover mainly depends on the diffused irradiance fraction.

* Corresponding author; e-mail: ponsathya@hotmail.com

Hence, for same irradiance conditions, the performance of the still varies place to place and day to day due to the changes in solar AOI and transmittance. The effect of this transmittance variation on the year round performance has not been discussed so far [3, 13-17]. The year round performance of the still in a particular place is mainly affected by the variations in transmittance of the covers and solar irradiance on the covers.

A single basin double slope solar still with basin area 1.7 m^2 was fabricated (still – solar), theoretically modeled (still – theoretical) and experiments were conducted with different energy absorbing materials and wick materials by the authors [8, 10]. Commercially available window glass was used as cover plate and its thickness was chosen as 4 mm to withstand the self-weight and thermal stresses. The inclination has been 30^o for maximum productivity [19]. The irradiance received by the inclined cover plate was taken as input to the still and the energy transmitted through the cover was calculated using the transmittance of the cover plates [12]. The global and diffused solar irradiances on horizontal plane and on the cover plate surfaces were estimated using ASHRAE [20] radiation model. In this work, using the experimental and theoretical data [7, 9, 11], the year round performance of the still for the year 2008 has been estimated for local place, National Engineering College, K. R. Nagar, Kovilpatti, India (9^{o}11'N, 77^{o}52'E).

Estimation of solar irradiance

As recommended by ASHRAE [20], hourly global irradiance (I), hourly direct irradiance (I_b) and hourly diffuse irradiance (I_d) on the horizontal surface on a clear day are calculated, using the equations:

$$I = I_b + I_d \tag{1}$$

$$I_b = B \sin\alpha \exp[-C/\sin\alpha)] \tag{2}$$

$$I_d = D\, I_{bn} \tag{3}$$

where B, C, and D are ASHRAE constants.

The angle between the sun rays and the horizontal plane (*i. e.* sun elevation angle α) and the angle between the sun rays and the vertical plane (*i. e.*, the AOI θ) can be calculated using the relation [21]:

$$\sin\alpha = \cos\phi \cos\delta \cos\omega + \sin\phi \sin\delta = \cos\theta \tag{4}$$

where $\phi = 9^o11'$ is the latitude of the National Engineering College, Kovilpatti, India; the sun declination (δ) is the angle between the sun's rays and the plane of the Earth's equator which varies with season for one year; the hour angle (ω) of the place is the angle through which the earth would turn to bring the meridian of the place directly under the sun. The sun elevation angle (α) and AOI (θ) are complementary angles.

The ASHRAE constants B, C, and D, predicted high values of the hourly direct irradiance and very low values of the hourly diffuse irradiance [22]. Hence, a procedure has been developed and the constants were evaluated by Parishwad *et al*. [22] for the estimation of direct, diffuse and global hourly solar irradiance on a horizontal surface for any location in India.

The method presented here was outlined by Liu and Jordon [23] and extended by Klein [24], to estimate the monthly mean daily irradiance on inclined planes. The global irradiance on the inclined plane, I_β, at an angle β is given by:

$$I_\beta = I_{\beta d} + I_{\beta b} + I_{g\text{-}r} \tag{5}$$

where $I_{\beta d}$, $I_{\beta b}$ and $I_{g\text{-}r}$ are the monthly mean hourly diffuse irradiance, direct irradiance and ground reflections, respectively, on the inclined plane at an angle β facing south or north. (South facing angles are positive and north facing angles are negative).

When the angle of inclination of the plane with the horizontal is at angle 'β' and facing south, the azimuth angle (θ_z) is given by [21]:

$$\cos\theta_z = \sin\delta\sin(\phi-\beta) + \cos\delta\cos(\phi-\beta)\cos\omega \tag{6}$$

when $\beta = 0$ and $\theta_z = \theta$.

The monthly mean hourly diffuse irradiance on the inclined plane, $I_{\beta d}$, is given by [25]:

$$I_{\beta d} = 0.5\, I_d\,(1 + \cos\beta) \tag{7}$$

The monthly mean hourly direct irradiance on the inclined plane, $I_{\beta b}$, is given by [25]:

$$I_{\beta b} = (I - I_d)\cos\theta_z/\cos\theta \tag{8}$$

where θ_z is the zenith angle calculated using the eq. (6).

The monthly mean hourly ground reflection on the inclined plane is given by [25]:

$$I_{g\text{-}r} = I\,\rho\, 0.5\,(1 - \cos\beta) \tag{9}$$

where, ρ is the ground albedo. For this work, ρ is taken as 0.2 assuming no snow condition [23]. Using the sun meter, this value is verified.

Theoretical analysis

The theoretical analysis of the still is done using the new model proposed by Kalidasa Murugavel *et al*. [8]. The total energy available for utilization by the still for given instant is the total irradiance transmitted (Q_t) through the covers for given time nd it is given by:

$$Q_t = Q_{tN} + Q_{tS} \tag{10}$$

where Q_{tN} (= $\tau_N A_{gN} I_N$) and Q_{tS} (= $\tau_S A_{gS} I_S$) are the irradiances transmitted through the north and south covers, τ_N and τ_S – the transmittances of the glass covers, A_{gN} and A_{gS} – the cover areas, and I_N and I_S – the incidence irradiances on the covers.

The global irradiance on the covers, I_N and I_S are calculated using the (5) to (9). τ_N and τ_S are calculated using the procedure explained in the references [8, 10, 12].

A part of irradiance transmitted into the still is absorbed by the basin and transferred to the water as heat ($Q_t\,\alpha_{bw}$). A part of this heat will be stored in the basin water ($m_w\, c_w\, dT_w/dt$) and feed water as sensible heat. A small quantity of heat is lost to atmosphere and remaining heat is transferred to glass through different modes. The transient energy balance equation for the basin water is given by:

$$Q_t\,\alpha_{bw} = m_w\, c_w \frac{dT_w}{dt} + Q_{c,w\text{-}g} + Q_{r,w\text{-}g} + Q_{e,w\text{-}g} + Q_{w\text{-}a} + Q_{fw} \tag{11}$$

where α_{bw} is the irradiance absorptivity of the basin water, m_w – the mass of water in the basin, c_w – the specific heat capacity of water, T_w – the basin water temperature, t – the time, $Q_{c,w\text{-}g}$ – the convection heat transfer from basin water to glass covers, $Q_{e,w\text{-}g}$ – the evaporation heat transfer from basin water to glass covers, $Q_{r,w\text{-}g}$ – the radiation heat transfer from basin water to glass covers, $Q_{w\text{-}a}$ – the heat loss from the basin to atmosphere, and Q_{fw} – the heat absorbed by the feed water.

The heat taken by the glass lower surface from basin water is transferred to the upper surface by conduction through the glass. The upper glass surface transfers this heat to atmosphere by convection and thermal radian due to the temperature difference between glass, atmosphere and sky. The temperature of glass material is assumed as constant throughout the material. It is also assumed that, the heat flow from the basin is uniform over the surface and both covers receive same amount of heat.

The transient energy balance equation for the glass cover is given by:

$$\alpha_g Q_i + Q_{c,w\text{-}g} + Q_{r,w\text{-}g} + Q_{e,w\text{-}g} = m_g c_g \frac{dT_g}{dt} + Q_{c,g\text{-}a} + Q_{r,g\text{-}sky} \quad (12)$$

where Q_i is the irradiance incidence on the inclined transparent covers, m_g – the mass of the glass covers, c_g – the specific heat capacity of the glass, T_g – the temperature of the glass, $Q_{c,g\text{-}a}$ – the heat convection heat transfer from glass to atmosphere, and $Q_{r,g\text{-}sky}$ – the heat transfer from glass to sky by radiation.

The instantaneous water production of the still is given by:

$$m_{w\text{-}c} = \frac{Q_{e,w\text{-}g}(t)}{h_{fg}} \quad (13)$$

where $m_{w\text{-}c}$ is the mass of water condensed, and h_{fg} – the latent heat of condensation of water.

For the local place Kovilpatti, the global and diffused irradiances falling on the horizontal surface were calculated using eqs. (1) to (4). The diffused irradiances received on the inclined covers were calculated using eqs. (5) to (9). The energy transmitted through the covers was calculated using eq. (10).

The theoretical performance of the still (here simply referred to as „still-theoretical") was evaluated by solving the heat balance eqs. (11) and (12). The different quantities used in the heat balance eqs. (11) and (12) were calculated by the procedure given by Malik *et al*. [2].

Since the basin and water temperatures, production rate of the still and instantaneous efficiency vary with time, a numerical approach was used for their calculations. For still – theoretical, the irradiance was calculated using the radiation model for every 10 seconds. The heat transfer coefficients were calculated using the initial values of water and glass temperatures, solar still parameters and other climatic conditions at 6 a. m. Using this heat transfer coefficients, values of basin and glass temperatures were calculated at the end 1of first interval of 10 seconds. Using these temperatures, heat transfer coefficients were calculated and the step was repeated to calculate the temperatures for the next interval. During the interval, the temperatures and climatic conditions were assumed to be constant. The fresh water production rate was calculated for each interval. The calculations were done for 24 hours duration starting from 6 a. m. for every first day of the month.

Table 1. Year round variation of temperatures and wind velocity at Kovilpatti

Month	Maximum temperature, [°C]	Minimum temperature, [°C]	Wind velocity, [ms^{-1}]
January	32.84	19.55	1.36
February	34.39	20.37	1.55
March	37.11	22.65	1.69
April	37.95	25.01	1.66
May	36.53	25.32	2.64
June	37.25	26.06	3.74
July	36.92	25.92	3.06
August	37.95	25.95	3.29
September	35.50	24.54	2.04
October	33.14	23.52	1.39
November	29.69	22.38	0.76
December	30.05	20.00	0.90

Table 1 shows the year round variations of minimal and maximal temperatures and wind velocity at Kovilpatti. The table is based on the meteorological data supplied by the Agricultural Research Centre, Tamil Nadu Agricultural University, Kovilpatti, for the five years from 2002 to 2006. The maximum temperature was higher and around 37 °C (98.6 °F) from March to August. In this period the minimal temperature was also high. The wind velocity was higher from June to August and minimal between November and December.

Experimental set-up and procedure

A single basin double slope solar still (here simply referred to as „still-solar“) was fabricated with mild steel plate as shown in fig. 1. The overall size of the basin is 2.3 m × 1 m × × 0.25 m. The bottom of the still was leveled with 5 cm thick concrete to minimize heat loss through the basin and to spread the water uniformly. The concrete surface was black painted to improve the irradiance absorption capacity. The top is covered with two glasses of thickness 4 mm inclined at 30° on both sides supported by wooden frame. The outer surfaces are covered with insulating glass wool and thermo cool layers. The condensed water is collected in the V-shaped drainage provided below the glass lower edge on both sides of the still. The condensate collected is continuously drained through flexible hose and stored in a measuring jar. A hole in the basin side wall allows inserting the thermocouples for the measurement of the basin water, still and condensate temperature. Four thermocouples were placed in the basin at different locations. Two thermocouples are placed in the each side of the drain to measure the condensate temperature. The hole is closed with insulating material to avoid the heat and vapor loss. Another hole is provided for water inlet. Through this hole, water tube from piezometer is inserted to supply raw water continuously to the basin from storage tank through control valves which regulates the flow, to keep the mass of water in the basin always constant.

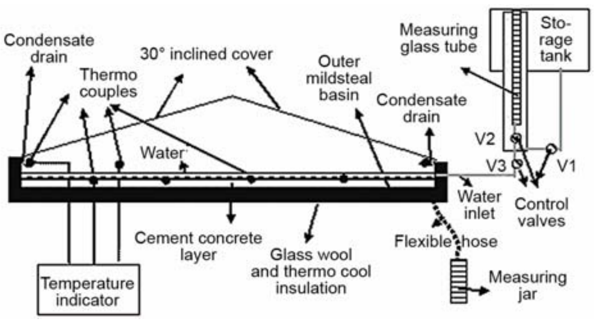

Figure 1. Single basin double slopes experimental still

The temperatures of water, and vapor were recorded with the help of calibrated K-type thermocouples in combination with a digital temperature indicator. The ambient temperature is measured by calibrated mercury thermometer. The distillate from the still was measured using a measuring jar. The raw water was supplied using measuring tube. The total and diffused irradiance on horizontal, inclined plane facing south and north were measured using a calibrated photovoltaic (PV) type sun meter. In this meter, the PV panel can be set at any inclination and orientation to measure the irradiance. This sun meter is calibrated frequently using the standard pyranometer available in our energy laboratory. The diffused irradiance on inclined surfaces was measured by blocking the direct irradiance on the PV surface. The wind velocity was measured with an electronic digital anemometer. Table 2 shows the accuracies and error for various instruments used. The maximum possible error occurred in any instrument is equal to the ratio between its least count and minimum value of the output measured.

The experiments were conducted at the open terrace of the Department of Mechanical Engineering during March 2008. Experiments were carried out for different depths from 0.5 cm to 6 cm. The observations were taken for 24 hours starting from 6 a. m., corresponding to the predicted data of the section above. The global and diffused irradiances on horizontal and irradiances on inclined planes, the temperatures of the atmosphere, condensate and basin water, and the masses of raw water supplied and condensate collected were recorded every 30 minutes.

Table 2. Accuracies and error for various measuring instruments

Instrument	Accuracy	Range	% error
Thermometer	±1 °C	0-100 °C	5%
Thermocouple	±0.1 °C	0-100 °C	0.5%
PV type sun meter	±1 W/m^2	0-1,500 W/m^2	2.5%
Anemometer	±0.1 m/s	0-15 m/s	10%
Measuring jar	±10 ml	0-1000 ml	10%
Measuring tube	±10 ml	0-500 ml	10%

Results and discussions

Figures 2(a) and (b) show the estimated year round variation of global solar irradiance. The north facing cover receives more global irradiance during March to May, while south facing cover receives more irradiance during October to March. In September, both covers receive the same amount of irradiance. During November to February, the south facing cover receives the irradiance close to normal during noon period with steep variation in incidence.

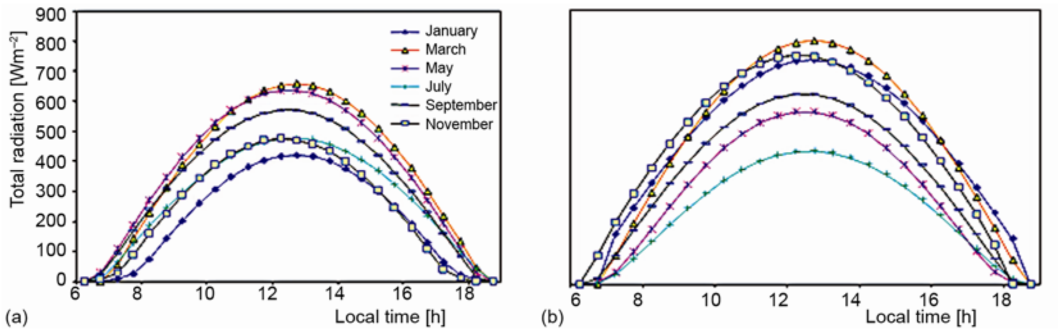

Figure 2. The total solar irradiance on north and south covers as a function of local time for various months for the year 2008 (for color image see journal web-site)

Figures 3 and 4 show the variation of the transmittance of the north and south facing covers, respectively, with local time for different months. The variation is opposite with the variation of AOI for most period of the day, since the transmittance is the function of AOI and diffused irradiance fraction for a given thickness. But, during morning and evening, transmittance values are higher due to the higher diffused fraction.

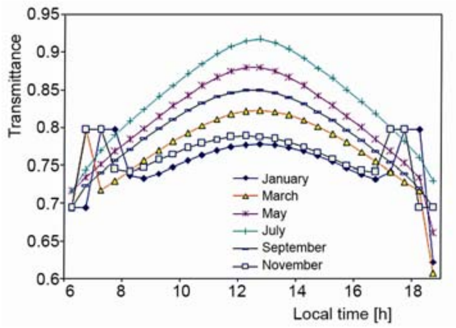

Figure 3. Transmittance variations – north cover for the year 2008
(for color image see journal web-site)

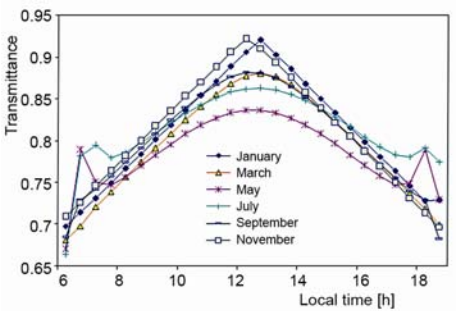

Figure 4. Transmittance variations – south cover for the year 2008
(for color image see journal web-site)

The comparison of theoretical and actual water temperatures is shown in fig. 5. At higher depth, the deviations between the theoretical and actual values are less. At lower depth, the deviation is higher. In the higher water temperature range, the deviations between the theoretical and actual values are higher. At higher water temperature, the water vapor proportion is high in the still air. This effect is not considered in the theoretical analysis. This is the reason for higher deviation between the theoretical and actual values. However, the variation pattern is similar for theoretical and experimental values.

Figure 6 shows the correlation between the still – theoretical and still – solar values. At lower water temperature, the model values are close to actual values. But at higher temperature, the deviation is higher. But in all ranges, the correlation coefficient between the actual and theoretical values is 0.933. The following correlation equation between actual and theoretical model water temperature can be used to estimate the actual temperature:

$$T_w(\text{actual}) = 0.6227\ T_w(\text{theoretical}) + 9.6183 \tag{14}$$

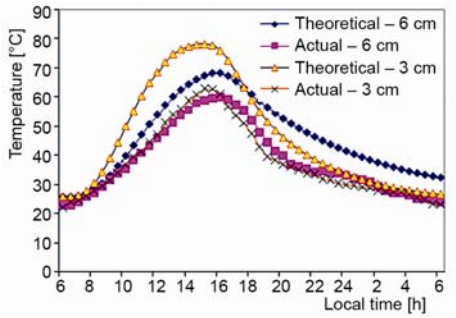

Figure 5. Actual and theoretical water temperature variations
(for color image see journal web-site)

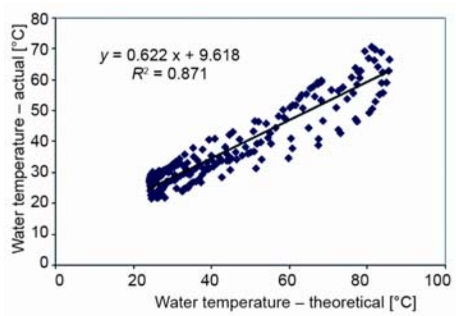

Figure 6. Correlation plot for water temperature
(for color image see journal web-site)

Figure 7 shows the comparison between the still – theoretical and still – solar glass temperatures. This variation is similar with water temperature. The reason for variation between the still – theoretical and still – solar is also same as for water temperature. The overall correlation coefficient is given by 0.921 as shown in fig. 8. The following correlation equation can be used, to estimate the glass temperature:

$$T_g(\text{actual}) = 0.5843\ T_g(\text{theoretical}) + 9.5516 \tag{15}$$

Figure 9 shows the comparison between the theoretical and actual production rate for the depths of 6 cm and 0.5 cm. The theoretical model [8] over predicts the production. At lower depth, the water temperature is high. At higher water temperature, the proportion of water vapor in the still air is high and this effect is not included in the theoretical model. This is the reason for higher deviation between theoretical and actual production rates at lower depth of 0.5 cm. From the performance study of the laboratory still and actual still [8], it is revealed that the production rate is a complex function of water and glass temperature and water – glass and glass – atmospheric temperature differences. Also for the higher water temperature, a different operation region is observed. During this region, the production rate is inversely proportional to the water – glass temperature difference. Hence another thermal model is required to predict the production rate accurately using the estimated temperatures.

A correlation developed [8] as thermal model (still – thermal) in terms of different temperatures is applied, for the accurate prediction of the production rate of the still. The correlation eqs. (14) and (15) can be used to estimate the water and glass temperatures.

The correlation [8] is applied for 4 cm, 3 cm, and 1 cm depths and validated during March 2007. Figure 10 shows the comparison between actual and thermal model. The thermal model predicted values are close to experimental values in all regions.

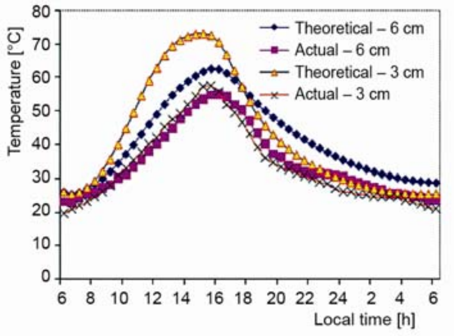

Figure 7. Actual and theoretical glass temperature variations
(for color image see journal web-site)

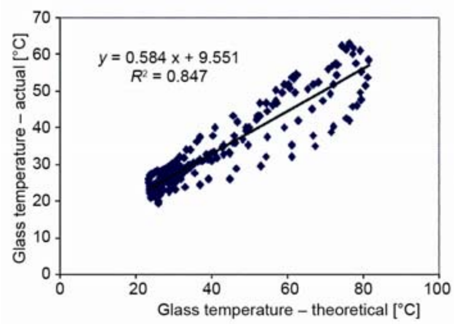

Figure 8. Correlation plot for glass temperature
(for color image see journal web-site)

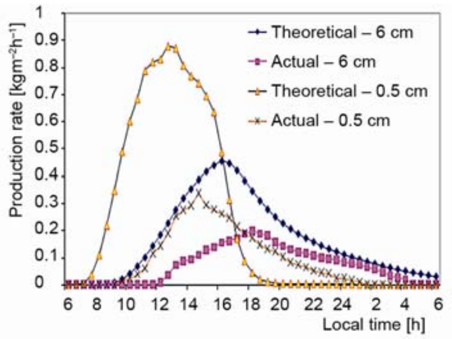

Figure 9. Actual and theoretical production rates
(for color image see journal web-site)

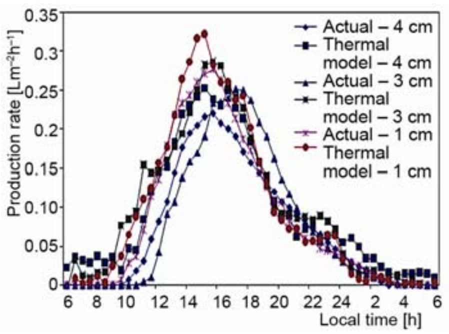

Figure 10. Actual and predicted production rate using thermal model – comparison
(for color image see journal web-site)

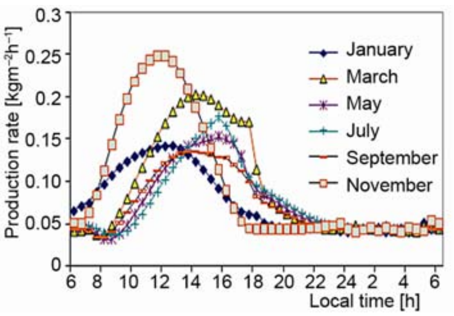

Figure 11. Variation of production rate for different months of the year 2008
(for color image see journal web-site)

Figure 11 shows the variation of production rate of the still for different months with local time for the still with 1 cm depth. In November, December, and March the production rate variation is on higher side. The variation pattern is different for different months. Higher slope variation occurs in March and November. Hence the rise in production rate is higher. In other months lower slope variations observed which show lower production rate. Similarly, the time for reaching maximum production rate is also different for different months. In November, the still reaches the maximum production rate point early around noon. For other months, still production rate reaches maximum after noon, with different time for different months. This is due to the variations in solar irradiance and atmospheric temperature. When solar intensity is higher and average atmospheric temperature is lower during a month, the still reaches maximum production rate point earlier during the day.

Figure 12 shows the overall production of the still for different months of the year. The still delivers around 4 L/day of water in March, April, August, November, and December.

For remaining months the still production varies between 3 to 4 L/day. In March and April, the solar energy received and transmitted by the covers are higher and hence the production is also higher. In November and December, the production rate is higher due to lower atmospheric temperature variation and lower wind velocity. In May, June, and July, the energy received and transmitted by the covers is minimum.

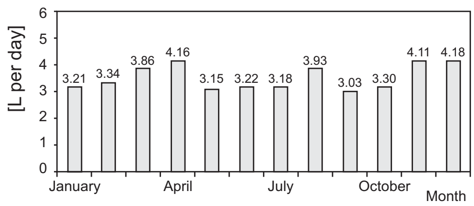

Figure 12. Overall production of the still as a function of months for the year 2008

Conclusions

In this work, a single basin double slope solar still is fabricated and tested. Theoretical and thermal models were used to predict the year round performance for the year 2008. ASHRAE [20] radiation model and meteorological data for the local place are used to estimate the irradiances received at the covers in different months. The production rate variations for different months have been studied as a function of local time. In November and March the variations are steeper. Similarly the time for maximum production rate is also different for different months. This is due to variations in irradiance incidence on the covers, atmospheric temperature and wind velocity. The overall production is higher in March, April, August, November and December and it is around 4 L/day. The average production of the still is 2.1 L/day/m^2.

Nomenclature

A – area, [m^2]
B – constants for given month, [Wm^{-2}]
C, D – constants
d – glass cover thickness, [mm]
dT – differential temperature, [^{o}C]
dt – differential time, [s]
h_{fg} – latent heat of water, [Jkg^{-1}]
I – hourly global irradiance, [Wm^{-2}]
K_d – diffused irradiance fraction
L – litre
m – mass, [kg]
m_{w-c} – mass flow rate of condensate, [kgs^{-1}]
Q – heat transfer rate, rate of energy, [W]
T – temperature, [^{o}C]
t – time, [s]

Greek symbols

α – solar altitude angle, [°]
α_b – absorptivity of the basin water
α_g – absorptivity of the glass
β – inclination of the cover with horizontal, [°]
Δ – difference
δ – sun declination angle, [°]
$\in$ – emissivity
θ – angle of incidence (AOI) , [°]
θ_z – zenith angle, incidence angle, [°]
ρ – ground albedo
τ – transmittance
Σ – algebraic sum
ω – hour angle, [°]
ϕ – latitude, [°]

Subscripts

a – air
b – basin, beam
bn – direct irradiance in the normal direction
c – convection
d – diffused
e – evaporation
fw – feed water
g – glass
g-r – ground reflection
i – incident
n – normal
N – north
r – irradiance
S – south
t – transmitted
w – water

Reference

[1] Kalidasa Murugavel, K., *et al*., Progresses in Improving the Effectiveness of the Single Basin Passive Solar Still, *Desalination, 220* (2008), 1-3, pp. 677–686
[2] Malik, M. A. S., *et al*., *Solar Distillation*, Pergamon press, Oxford, UK, 1982

[3] Singh, H. N., Tiwari, G. N., Monthly Performance of Passive and Active Solar Stills for Different Indian Climatic Conditions, *Desalination, 168* (2004), 15, pp. 145-150
[4] Velmurugan, V., *et al*., Productivity Enhancement of Stepped Solar Still – Performance Analysis, *Thermal Science, 12* (2008), 3, pp. 153-163
[5] Feilizadeh, M., *et al*., A New Radiation Model for a Single-Slope Solar Still, *Desalination, 262* (2010), 1-3, pp. 166-173
[6] Madhlopa, A., Johnstone, C. M., Computation of Solar Radiation Distribution in a Solar Still with Internal and External Reflectors, *Solar Energy, 85* (2011), 2, pp. 217-233
[7] Arjunan, T. V., *et al*., Effect of Sponge Liner on the Internal Heat Transfer Coefficients in a Simple Solar Still, *Desalination and Water Treatment, 29* (2011), 1, pp. 271-284
[8] Kalidasa Murugavel, K., *et al*., Single Basin Double Slope Solar Still with Minimum Basin Depth and Energy Storing Materials, *Applied Energy, 87* (2010), 2, pp. 514-523
[9] Eduardo Rubio, Fernandez, J. L., Porta-Gandara, M. A., Modeling Thermal Asymmetries in Double Slope Solar Stills, *Renewable Energy, 29* (2004), 6, pp. 895-906
[10] Kalidasa Murugavel, K., Srithar, K., Performance Study on Basin Type Double Slope Solar Still with Different Wick Materials and Minimum Mass of Water, *Renewable Energy, 36* (2011), 2, pp. 612-620
[11] Hiroshi, T., A Theoretical Analysis of Basin Type Solar Still with Flat Plate External Bottom Reflector, *Desalination, 279* (2011), 1-3, pp. 243-251
[12] Kalidasa Murugavel, K., *et al*., Experimental Analysis on Variation of Transmittance of Different Thickness Window Glasses at Different Solar Insolation Conditions, 3rd BSME-ASME International Conference on Thermal Engineering, Dhaka, Bangladesh, B. A. 048 (2006), http://bsmeicte2012.iutoic-dhaka.edu/proceedings/3rd-bsme-asme-icte-2006/html/indexret-.htm
[13] Kabeel, A. E., El-Agouz, S. A., Review of Researches and Developments on Solar stills, *Desalination, 276* (2011), 1-3, pp. 1-12
[14] Singh A. K., Tiwari, G. N., Long-Term Comparative Study of Solar-Distiller Systems, *Energy, 18* (1993), 11, pp. 1161-1169
[15] El-Sebaii, A. A., *et al*., Year-Round Performance of a Modified Single-Basin Solar Still with Mica Plate as a Suspended Absorber, *Energy, 25* (2000), 1, pp. 35-49
[16] AI-Hinai, H., *et al*., Parametric Investigation of a Double-Effect Solar Still in Comparison with a Single-Effect Solar Still, *Desalination, 150* (2002), 1, pp. 75-83
[17] Abu-Arabi, M., Zurigat, Y., Year-Round Comparative Study of Three Types of Solar Desalination Units, *Desalination, 172* (2005), 2, pp. 137-143
[18] Abdul Jabbar, N. *et al*, Experimental Study on the Effect of Internal and External Reflectors on the Performance of Basin Type Solar Stills at Various Seasons, *Desalination and Water Treatment, 27* (2011), 1-3, pp. 313-318
[19] Tiwari, A. K., Tiwari, G. N., Effect of the Condensing Cover's Slope on Internal Heat and Mass Transfer in Distillation: an Indoor Simulation, *Desalination, 180* (2005), 1-3, pp. 73-88
[20] ***, *ASHRAE Handbook of Fundamentals*, American Society of Heating, Refrigeration and Air-Conditioning Engineers, Atlanta, Geo., USA, 1985
[21] Duffie, J. A., Beckman, W. A., *Solar Engineering of Thermal Processes*, 3rd edition, John Wiley and Sons, New York, USA, 2006
[22] Parishwad, G. V., *et al*., Estimation of Hourly Solar Radiation for India, *Renewable Energy, 12* (1997), pp. 303-313
[23] Liu, B. Y. H., Jordan, R. C., The Interrelationship and Characteristic Distribution of Direct, Diffuse and Total Solar Radiation, *Solar Energy, 4* (1960), 3, pp. 1-19
[24] Klein, S. A., Calculation of Monthly Average Insolation on Tilted Surfaces, *Solar Energy, 23* (1977), 6, pp. 526-541
[25] Anna Mani, *Handbook of Solar Radiation Data for India*, Allied publishers Private Limited, Chennai, Tamil Nadu, India, 1980

Paper submitted: May 17, 2012
Paper revised: July 26, 2013
Paper accepted: July 26, 2013